ISSN: 1410-8917
e-ISSN: 2597-9914

Jurnal Kimia Sains dan Aplikasi 29 (7) (2026): 491-504

Jurnal Kimia Sains dan Aplikasi
Journal of Scientific and Applied Chemistry

Journal homepage: http://ejournal.undip.ac.id/index.php/ksa

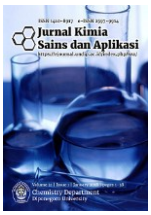

Bioactivity Profile, Toxicity Screening, and Biopolymer Film Application of Biosynthesized Silver Nanoparticles from *Trema orientalis* Leaf Extract

Aghniya Naziefa, Rahmiwati Hilma *, Mustika Widuri Bulan, Dwi Rosalinda, Jufrizal Syahri

Department of Chemistry, Faculty of Mathematics, Natural Sciences and Health, Universitas Muhammadiyah Riau, Pekanbaru, Indonesia

* Corresponding author: rahmiwatihilma@umri.ac.id

https://doi.org/10.14710/jksa.29.7.491-504

Article Info

Article history:

Received: 21st May 2026
Revised: 21st July 2026
Accepted: 27th July 2026
Online: 31st August 2026

Keywords:
Silver Nanoparticle; *Trema orientalis* Leaf Extract; Food Packaging; Antioxidant; Antiphotooxidation

Abstract

This study utilizes green nanotechnology by employing *Trema orientalis* leaf extract (TO-EE) as a natural bioreductant to synthesize silver nanoparticles (AgNPs-TO) and apply them in biopolymer film-based food packaging. AgNPs were synthesized using a stirrer method and characterized by UV-Vis, FTIR, XRD, PSA, and TEM. UV-Vis confirmed nanoparticle formation with a λ_{max} at 430 nm (SPR). FTIR indicated phenolic and carbonyl groups in the reduction of Ag^{+} to Ag^{0}. XRD showed a face-centered cubic silver structure with minor AgCl presence. PSA revealed an average size of 56.46 nm with high polydispersity (>0.5), while TEM showed spherical, heterogeneous particles. Antioxidant activity (DPPH) showed IC_{50} values of 128.40 µg/mL (AgNPs-TO) and 75.59 µg/mL (TO-EE). Anti-photooxidation tests in a linoleic acid system demonstrated that AgNPs-TO and BP/AgNPs-TO films suppressed hydroperoxide formation. Preliminary BSLT screening showed an LC_{50} <1000 ppm, and 5 ppm AgNPs were selected for incorporation into the biopolymer film. The additional AgNPs-TO also affects the physical properties of the biopolymer film. These results indicate that AgNPs-TO are promising as active agents in environmentally friendly food packaging.

1. Introduction

Food demand continues to increase along with the growth of Indonesia's population. Based on the 2022 Food Security Statistics, Indonesia ranked 63rd out of 113 countries, with a Global Food Security Index (GFSI) score of 60.2 [1]. Indicating a relatively lower position compared to other Southeast Asian countries. This condition highlights the importance of strengthening food security, especially in terms of food utilization, which includes aspects of quality and safety, as these are directly related to public consumption patterns [2].

One of the factors influencing food quality and safety is exposure to light and ultraviolet (UV) radiation. Such exposure can trigger photooxidation processes that lead to a decline in food quality and the degradation of essential nutrients. Light and UV radiation promote the formation of highly reactive species, such as hydroxyl radicals and Reactive Oxygen Species (ROS), which can damage vitamins, pigments, lipids, and oils in food [3]. Herefore, packaging plays an essential role in protecting food products from external factors, including light and humidity, thereby extending shelf life and preserving product quality.

Current food packaging systems predominantly utilize petroleum-based plastics and their composites. However, these materials are generally transparent and offer limited protection against light exposure unless modified with additional components or additives [4]. This limitation necessitates the development of innovative materials or active agents that can be incorporated into packaging systems to enhance protection against food deterioration. One promising approach involves the application of nanotechnology, particularly the use of nanoparticles. Nanoparticles are characterized by their extremely small size, typically

ranging from 1 to 100 nm, and are often synthesized from metals such as silver, gold, palladium, and selenium [5].

Among various metal-based nanoparticles, silver nanoparticles have attracted considerable attention due to their distinctive physical, chemical, and biological properties. These include high electrical and thermal conductivity, notable optical characteristics, nonlinear catalytic behavior, and significant biochemical activity, which enable their wide-ranging applications across multiple fields [5].

Silver nanoparticles have been widely reported to exhibit diverse biological activities, including antibacterial, antiviral, antioxidant, antidiabetic, anticancer, and antifungal effects [6]. The antioxidant activity of green-synthesized AgNPs is primarily associated with surface-bound phytochemicals, particularly phenolic and flavonoid compounds, which act as capping agents capable of donating hydrogen atoms or electrons to neutralize free radicals. The metallic silver core itself is not the primary free radical scavenger. Furthermore, they have demonstrated effectiveness as protective agents against ultraviolet (UV) radiation [7].

Silver nanoparticles can be synthesized through physical and chemical approaches; however, these methods often require harsh conditions and may pose environmental concerns. In recent years, biological or green synthesis methods have attracted increasing attention due to their cost-effectiveness and relatively simple procedures. Moreover, these approaches are considered more environmentally sustainable, as they typically employ natural resources such as plant extracts as bioreducing agents in the nanoparticle formation process [8].

One plant that has potential for use in the synthesis of silver nanoparticles (AgNPs) is *Trema orientalis* (Mengkirai). This plant has been reported to exhibit various biological activities, including antioxidant, antibacterial, antidiabetic, and anti-inflammatory properties. In addition, the leaves of *T. orientalis* are known to contain a range of secondary metabolites, such as tannins, flavonoids, saponins, terpenoids, glycosides, and carbohydrates [9]. Previous studies [10] have successfully synthesized green AgNPs using *T. orientalis* and evaluated their antibacterial activity.

In addition, Gudimalla *et al.* [11] and Balciunaitiene *et al.* [12] have reported the green synthesis of AgNPs for incorporation into polymer films and evaluated their antibacterial and antioxidant activities. However, the application of *T. orientalis*-mediated AgNPs in alginate-based biopolymer films remains relatively limited, particularly regarding their antioxidant and anti-photooxidative activities and their potential application in active food packaging systems. Therefore, this study aims to investigate the bioactivity profile of biosynthesized silver nanoparticles, including their antioxidant and anti-photooxidation activities, along with toxicity assessment and their potential application in active food packaging systems using *T. orientalis* leaf ethanol extract (TO-EE) as the functional component.

2. Experimental

2.1. Equipment and Materials

The equipment used in this study included an analytical balance (Shimadzu), a rotary evaporator (Buchi), a distillation apparatus, 10-1000 µL micropipettes, an oven (Memmert), a microplate reader, glassware in the chemistry laboratory, a UV-Vis spectrophotometer (Shimadzu), a light box, and a 22-watt LED lamp. Characterization was performed using LC-MS (Lab Reserse POLDA Metrojaya), TEM and PSA (PPNN ITB Electron Microscopy Lab), FTIR and XRD (UNP Chemistry Lab).

The materials used in this study were mengkirai leaves (*T. orientalis*) collected in Pekanbaru, technical ethanol, $AgNO_3$ (Merck), DPPH (Sigma-Aldrich), ascorbic acid (Merck), distilled water, seawater, *Artemia salina* larvae, HCl (Merck), Meyer's reagent, Lieberman-Burchard's reagent, linoleic acid, erythrosine, Tween 20, Mg powder, ethanol (pro-analysis), methanol (pro-analysis; Merck), Gallic acid, Folin-Ciocalteu (Sigma-Aldrich), sodium alginate, PEG-400, and $CaCl_2$.

2.2. Preparation of TO-EE Sample and Phytochemical Screening Test

A total of 5 kg of mengkirai leaves *(T. orientalis)* were collected in the vicinity of the Universitas Muhammadiyah Riau in Pekanbaru, Riau. The samples were thoroughly washed and air-dried without exposure to direct sunlight. Once dry, the leaves were ground into a crude powder weighing 500 g (10%). The extraction process was performed using the maceration method with ethanol as the solvent at a 1:4 ratio. The mixture was stored in a dark container for 3 × 24 hours with occasional stirring. Afterward, the macerate was filtered, and the residue was re-extracted by adding the same solvent for 24 hours, then filtered again. All the filtrate obtained was then concentrated using a rotary evaporator to produce 82.29 g (16.45%) of TO-EE. Subsequently, the TO-EE underwent phytochemical screening for alkaloids, flavonoids, steroids/terpenoids, phenolics, tannins, and saponins [13]. Subsequently, the TO-EE was characterized using LC-MS spectroscopy.

2.3. Molecular Docking

The crystal structure of KEAP1 (PDB ID: 4L7B) was obtained from the RCSB Protein Data Bank. Protein preparation was carried out by separating the co-crystallized ligand from the receptor structure using UCSF Chimera. The extracted ligand was then re-docked into the original binding pocket using AutoDock Vina to validate the docking protocol [14]. Validation was performed by determining the root mean square deviation (RMSD) between the experimental ligand pose and the re-docked conformation in PyMOL. A docking protocol was considered acceptable when the RMSD value was below 2.0 Å [15]. Following successful validation, the compounds identified in TO-EE by LC-MS analysis were docked into the validated binding pocket of KEAP1. The binding affinity values (kcal/mol) obtained from AutoDock Vina were subsequently used to evaluate the ligand–protein interactions.

2.4. Determination of Total Phenolic Content of TO-EE

The obtained TO-EE was subsequently analyzed for its total phenolic content. A gallic acid stock solution (1000 ppm) was prepared by dissolving 0.025 g of gallic acid in a 25 mL volumetric flask. Standard solutions were then prepared from this stock at concentrations of 50, 100, 150, 200, and 250 ppm. For the assay, 0.5 mL of 2.5 N Folin Ciocalteu reagent was added to each standard solution, followed by vortex mixing and incubation for 5 minutes. Subsequently, 2.5 mL of 7.5% Na_2CO_3 solution was added. The absorbance of each solution was measured using a UV–Vis spectrophotometer at a maximum wavelength of 765 nm. For the TO-EE sample, a solution with a concentration of 1 mg/mL was prepared and treated using the same procedure as the standard solutions. The reaction resulted in a yellowish-blue color change.

2.5. Synthesis of AgNPs Using TO-EE as Reducing Agent (AgNPs-TO)

The 1 mM $AgNO_3$ solution and TO-EE solutions at concentrations of 0.5%, 1%, and 1.5% were prepared. Subsequently, the $AgNO_3$ solution was mixed with each TO-EE solution at a ratio of 1:10 (v/v). The mixtures were then stirred continuously on a hotplate stirrer at 60°C for 60 minutes, until a yellowish-brown color change was observed, indicating nanoparticle formation. The resulting products were characterized using UV–Vis spectrophotometry to confirm the formation of AgNPs, as indicated by the presence of surface plasmon resonance (SPR) absorption peaks within the wavelength range of 400–450 nm [16]. The optimum TO-EE concentration was determined based on the UV–Vis spectral characteristics of the resulting AgNPs.

2.6. Determination of Antioxidant Activity (DPPH)

Antioxidant activity was evaluated using the DPPH method. A DPPH solution was prepared at a concentration of 80 µg/mL in methanol. Ascorbic acid (vitamin C) stock solution was prepared at 1000 µg/mL and subsequently diluted to 100 µg/mL. TO-EE and AgNPs-TO solutions were prepared at six concentrations: 100, 50, 25, 12.5, 6.25, and 3.125 µg/mL. The assay was conducted using a 96-well microplate reader. A 100 µL aliquot of each sample solution (TO-EE, AgNPs-TO, and vitamin C) at its respective concentration was mixed with 100 µL of DPPH solution in each well. The mixtures were incubated for 30 minutes at room temperature under dark conditions. Absorbance was measured at a wavelength of 517 nm, and all measurements were performed in triplicate. The percentage of inhibition and IC_{50} values were subsequently calculated by Equation 1 [17].

$$\%Inhibition = \frac{A_{control} - A_{sample}}{A_{control}} \times 100\% \quad (1)$$

2.7. Brine Shrimp Lethality Test (BSLT) for Toxicity Evaluation

Approximately 100 mg of *Artemia salina* eggs were incubated in 1 L of seawater in a compartmentalized aquarium with illuminated and dark sections separated by a perforated barrier. The illuminated section was exposed to a light source and supplied with continuous aeration, while the dark section was kept covered. After 48 hours, the newly hatched nauplii were collected and utilized for toxicity assessment. A negative control was prepared, and 100 mg of TO-EE was dissolved in seawater to obtain the test solution. Serial concentrations of 100, 250, 500, 750, and 1000 µg/mL were prepared and adjusted to a final volume of 5 mL using seawater as the diluent. AgNPs-TO samples were similarly prepared at concentrations of 2.5, 5, 10, 25, and 50 µg/mL. Each concentration, including the control, was tested in triplicate in vials containing 10 nauplii. Following a 24-hour incubation period, the number of surviving larvae was recorded. Toxicity data were subsequently analyzed to determine the LC_{50} using probit analysis of the percentage mortality, as described in Equation 2.

$$\%Mortality = \frac{Number\ of\ dead\ larvae}{Total\ number\ of\ larvae\ at\ the\ start} \times 100\% \quad (2)$$

Subsequently, a linear regression equation was obtained describing the relationship between probit values and the logarithm of concentration, where the Y variable represents the probit value and the X variable represents the logarithm of concentration [18].

2.8. Antiphotooxidation Activity Test

The antiphotooxidation activity was evaluated using linoleic acid [19]. An emulsion system with a total volume of 5 mL was prepared by gradually combining linoleic acid, Tween 20, and distilled water to maintain consistent concentration ratios. AgNPs-TO samples at concentrations of 5, 10, and 15 ppm, along with BP/AgNPs-TO at concentrations of 0, 5, and 10 ppm, were subsequently incorporated into the emulsion, followed by the addition of erythrosine. The prepared mixtures were then irradiated with a 22 W LED lamp for 5 hours, with observations recorded hourly. The formation of conjugated diene hydroperoxides was analyzed by taking 30 µL of the emulsion, adding 5 mL of absolute ethanol, and measuring the absorbance at 232 nm [20].

2.9. Film Preparation

Biopolymer films were prepared with modifications to a previously reported method [21] using sodium alginate as the base material and polyethylene glycol (PEG-400) as a plasticizer. A film-forming solution was prepared by dissolving sodium alginate in distilled water at a concentration of 3% (b/v), followed by the addition of 0.5 mL PEG-400. BP/AgNPs-TO samples were incorporated at varying AgNP concentrations of 0, 5, 10, and 25 ppm. The mixture was then stirred using a hotplate stirrer until a homogeneous solution was obtained. The resulting solution was cast evenly onto a mold and dried in an oven at 60°C for 8 hours. After drying, the films were allowed to cool at room temperature and subsequently treated with 0.5% $CaCl_2$ solution as a crosslinking agent. The films were then further dried at room temperature for 24 hours.

2.10. Characterization of Biopolymer Films (BP/AgNPs-TO)

The thickness of BP/AgNPs-TO films was determined with a caliper at three different points, and the average was calculated. Water absorption was

evaluated by cutting the BP/AgNPs-TO films into dimensions of 1 × 3 cm. The samples were first weighed using an analytical balance after being stored in a desiccator to obtain the initial weight (W_1). Each sample was then immersed in a petri dish containing 10 mL of distilled water for 1 minute. After immersion, excess surface water was carefully removed using tissue paper, and the samples were reweighed to obtain the final weight (W) [22]. It was calculated according to Equation 3.

$$Water\ absorption\ (\%) = \frac{W-W_1}{W_1} \times 100\% \quad (3)$$

Where, W_1 represents the starting sample weight (g), and W represents the final sample weight (g) [23].

Subsequently, the tensile strength of BP/AgNPs-TO films was evaluated. The samples were cut into dimensions of 3×15 cm and clamped at both ends along their length. After testing, the applied force and elongation were recorded. The tensile strength was calculated as the ratio of the maximum force at break (F) to the initial cross-sectional area. The initial cross-sectional area was determined by multiplying the initial thickness (a) by the initial width (b). The results were expressed in units of MPa (N/mm²) [24].

3. Results and Discussion

3.1. Phytochemical Screening

The results of the phytochemical screening of the TO-EE extract indicate that the extract contains flavonoids, alkaloids, saponins, steroids, and phenolic compounds, as shown in Table 1. The presence of these compounds supports the extract's potential as an active ingredient in the production of active packaging, as it can provide bioactivity, particularly antioxidant activity. This is consistent with previous studies reporting by Taiwo *et al.* [25], that TO-EE contains secondary metabolites such as tannins, phenols, flavonoids, and saponins. LC-MS characterization further revealed 16 compounds in TO-EE, including phenolic and phenolic glycoside compounds, which are capable of reducing Ag^+ to Ag^0 during the synthesis of silver nanoparticles. LC-MS analysis of TO-EE resulted in a chromatogram with several peaks, indicating the presence of bioactive compounds in the extract, as shown in Figure 1. For further details on the TO-EE compound results from the LC-MS chromatogram, see Table 2.

Table 1. Results of the phytochemical analysis of the TO- EE

Compound class	Reagents	Result
Flavonoids	HCl + Mg	(+)
Saponins	Distilled water	(+)
Terpenoids/Steroids	Liberman Burchad	(+) Steroid
	Mayer	(+)
Alkaloids	Wagner	(-)
	Dragendrof	(-)
Phenolics	$FeCl_3$	(+)
Tannins	$FeCl_3$ + H_2SO_4	(+)

(+): Contains the compound, (-): Does not contain the compound

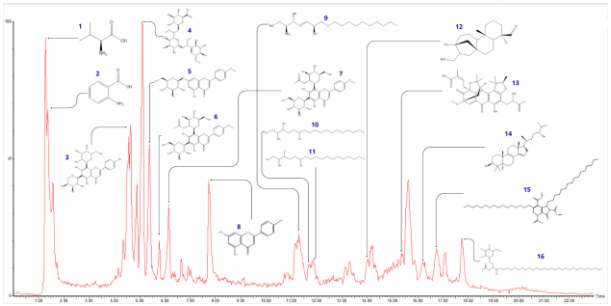

Figure 1. The LC-MS spectrum results of TO-EE

3.2. Molecular Docking Result

The molecular docking protocol was successfully validated by re-docking the co-crystallized native ligand into the binding site of Keap1 (PDB ID: 4L7B). The superimposition of the crystallographic and re-docked ligand conformations is presented in Figure 2. The RMSD value obtained was 0.670 Å, which was well below the acceptable threshold of 2.0 Å [15], indicating excellent agreement between the experimental and predicted ligand conformations. This result confirmed that the docking protocol was sufficiently accurate and reliable for subsequent molecular docking analysis.

Following the successful validation of the docking protocol, all compounds identified by LC–MS were docked into the active site of Keap1 (PDB ID: 4L7B). Keap1 is a key regulator of the Nrf2 signaling pathway involved in cellular antioxidant defense. Under normal conditions, Keap1 binds to Nrf2 and promotes its degradation. Inhibition of Keap1 releases Nrf2, allowing it to activate antioxidant-related genes such as HO-1 and NQO1 [26]. The molecular docking results are summarized in Table 3. Binding affinity represents the predicted strength of interaction between a ligand and the target protein, where more negative values indicate stronger and more stable ligand–protein interactions.

As shown in Table 3, the binding affinity values ranged from -4.59 to -10.41 kcal/mol. Among the identified compounds, compound 5 exhibited the strongest predicted binding affinity toward Keap1 (-10.41 kcal/mol), followed by compound 3 (-9.49 kcal/mol) and compound 4 (-8.95 kcal/mol). These values were lower than those of the positive control, ascorbic acid (-6.24 kcal/mol), indicating stronger predicted interactions with the Keap1 binding site, whereas compound 1 showed the weakest binding affinity (-4.59 kcal/mol).

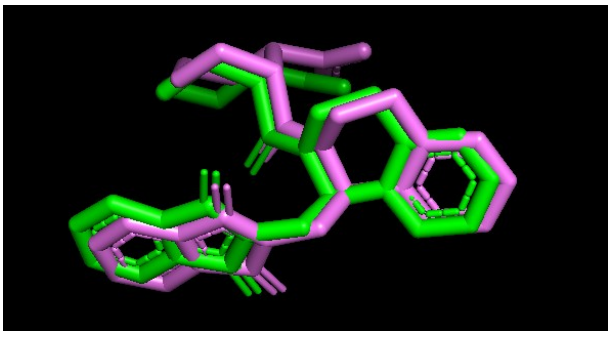

Figure 2. Superimposition of the crystallographic (native) ligand (purple) and the re-docked ligand (green) in the active binding site of Keap1 (PDB ID: 4L7B)

Table 2. TO-EE compounds

No.	RT (min)	Chemical formula	Mol weight (g/mol)	Compound name	Structure
1	1.28	$C_5H_{11}NO_2$	117.15	Essential amino acid L-Valine	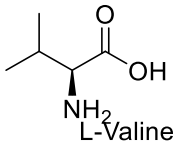 L-Valine
2.	1.37	$C_7H_7NO_2$	137.14	Aromatic amino acid Anthranilic acid	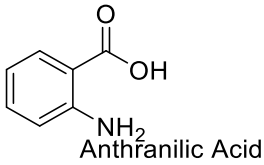 Anthranilic Acid
3.	4.64	$C_{26}H_{28}O_{14}$	564.5	Flavonoid Isoschaftoside	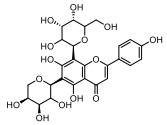 5,7-dihydroxy-2-(4-hydroxyphenyl)-8-[(2S,4S,5S)-3,4,5-trihydroxy-6-(hydroxymethyl)tetrahydropyran-2-yl]-6-[(2S,4S,5S)-3,4,5-trihydroxytetrahydropyran-2-yl]chromen-4-one
4.	5.12	$C_{21}H_{36}O_{19}$	592.5	Oligosaccharide	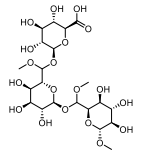 (2S,3S,4S,5R,6S)-3,4,5-trihydroxy-6-[[(2R,3R,4S,5R,6S)-3,4,5-trihydroxy-6-[[(2R,3S,4S,5R,6R)-3,4,5-trihydroxy-6-methoxyoxan-2-yl]methoxymethoxy]oxan-2-yl]methoxymethoxy]oxane-2-carboxylic acid
5.	5.39	$C_{22}H_{22}O_{10}$	446.4	Flavonoid glycoside Tilianin	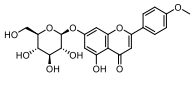 5-hydroxy-2-(4-methoxyphenyl)-7-[(2S,3R,4S,5S,6R)-3,4,5-trihydroxy-6-(hydroxymethyl)oxan-2-yl]oxychromen-4-one
6	5.79	$C_{30}H_{34}O_{16}$	650.6	Flavonoid glycoside Tremasperin (Trema compound)	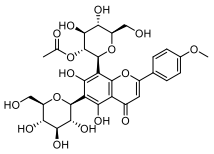 [(2S,3R,4S,5S,6R)-2-[5,7-dihydroxy-2-(4-methoxyphenyl)-4-oxo-6-[(2S,3R,4R,5S,6R)-3,4,5-trihydroxy-6-(hydroxymethyl)oxan-2-yl] chromen-8-yl]-4,5-dihydroxy-6-(hydroxymethyl)oxan-3-yl] acetate
7	6.16	$C_{30}H_{34}O_{16}$	650.6	Flavonoid glycoside Tremasperin (Trema compound)	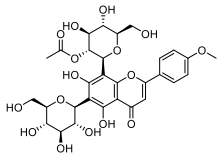 [(2S,3R,4S,5S,6R)-2-[5,7-dihydroxy-2-(4-methoxyphenyl)-4-oxo-6-[(2S,3R,4R,5S,6R)-3,4,5-trihydroxy-6-(hydroxymethyl)oxan-2-yl]chromen-8-yl]-4,5-dihydroxy-6-(hydroxymethyl)oxan-3-yl] acetate
8	7.73	$C_{15}H_{10}O_5$	271.24	Flavonoid Apigenin	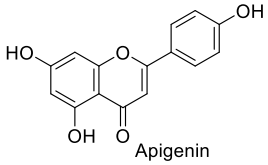 Apigenin
9	11.31	$C_{18}H_{37}NO_3$	315.5	Sphingoid	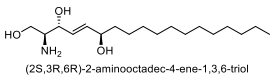 (2S,3R,6R)-2-aminooctadec-4-ene-1,3,6-triol
10	11.71	$C_{18}H_{39}NO_3$	317.5	Sphingoid	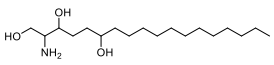 6-Hydroxy dihydrosphingosine
11	11.85	$C_{18}H_{39}NO_3$	317.5	Sphingoid	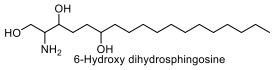 6-Hydroxy dihydrosphingosine
12	14.11	$C_{20}H_{32}O_2$	304.5	Terpenoid > Diterpenoid	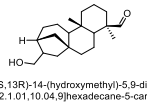 (1S,5R,9S,13R)-14-(hydroxymethyl)-5,9-dimethyltetracyclo[11.2.1.01,10.04,9]hexadecane-5-carbaldehyde

No.	RT (min)	Chemical formula	Mol weight (g/mol)	Compound name	Structure
13	15.37	$C_{34}H_{40}O_{10}$	608.26215	Flavonoid Scortechinone R	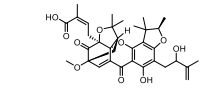 (Z)-4-[(1R,2R,7R,16S,18S)-11-hydroxy-10-(2-hydroxy-3-methylbut-3-enyl)-16-methoxy-6,6,7,20,20-pentamethyl-13,17-dioxo-3,8,19-trioxahexacyclo [14.4.1.02,14.02,18.04,12.05,9] henicosa-4(12),5(9),10,14-tetraen-18-yl]-2-methylbut-2-enoic acid
14	16.20	$C_{29}H_{48}O_2$	428.7	Steroid	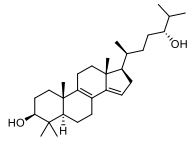 (3S,5R,10S,13R,17R)-17-[(2S,5R)-5-hydroxy-6-methylheptan-2-yl]-4,4,10,13-tetramethyl-1, 2,3,5,6,7,11,12,16,17-decahydrocyclopenta[a]phenanthren-3-ol
15	16.75	$C_{46}H_{79}NO_6$	742.1	Indanone	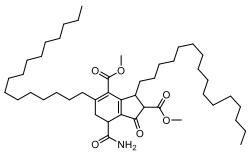 Dimethyl 7-carbamoyl-3,5-dihexadecyl-1-oxo-2,3,6,7-tetrahydroindene-2,4-dicarboxylate
16	17.75	$C_{40}H_{79}NO_8$	702.1	Lipid > Ceramide glycoside	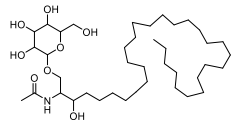 N-[3-hydroxy-1-[3,4,5-trihydroxy-6-(hydroxymethyl)oxan-2-yl]oxydotriacontan-2-yl]acetamide

Table 3. Molecular docking results of the identified compounds against Keap1 (PDB ID: 4L7B)

Ligand	Binding affinity (kcal/mol)	Ligand	Binding affinity (kcal/mol)
Ascorbic acid	-6.24	Compound 9	-6.16
Compound 1	-4.59	Compound 10	-6.31
Compound 2	-5.61	Compound 11	-6.30
Compound 3	-9.49	Compound 12	-8.02
Compound 4	-8.95	Compound 13	-8.71
Compound 5	-10.41	Compound 14	-8.55
Compound 6	-7.88	Compound 15	-6.60
Compound 7	-7.90	Compound 16	-6.80
Compound 8	-8.77		

3.3. Total Phenolic Content Test Results

TO-EE was analyzed for total phenolic content using the Folin–Ciocalteu method, with gallic acid serving as the standard reference. A calibration curve of gallic acid was constructed to establish the relationship between concentration and absorbance, yielding the equation $y = 0.0024x + 0.0129$ with an R^2 value of 0.998.

During the assay, the reaction between gallic acid and the Folin–Ciocalteu reagent initially produced a yellow coloration, indicating the presence of phenolic compounds. Upon the addition of Na_2CO_3, the solution changed to blue. The absorbance of TO-EE was measured in triplicate, and the average value was used to calculate the total phenolic content. The results were expressed as milligrams of gallic acid equivalents (mg GAE), representing the equivalent amount of gallic acid per gram of sample [27]. The total phenolic content of TO-EE was determined to be 168.9722 mg GAE/g of extract, as shown in Table 4.

3.4. Results of AgNPs-TO Synthesis

3.4.1. Results of UV-Vis Spectrophotometry Characterization

The results of the synthesis of AgNPs from mengkirai leaf extract were analyzed using UV-Vis spectroscopy by observing the peak wavelengths that appeared. The synthesis was carried out by mixing 50 mL of 1 mM $AgNO_3$ solution and 5 mL of extract solution at varying concentrations of 0.5%, 1%, and 1.5%, using a stirrer for 60 minutes at 60°C, as shown in Figure 4. The best peak results were obtained at concentrations of 0.5% and 1%, specifically at wavelengths of 400–450 nm. The optimal wavelength, with the highest peak, was observed at 430 nm in the 1% extract concentration. This is consistent with existing research indicating that silver nanoparticles exhibit strong absorbance at wavelengths between 400 and 500 nm [28]. In addition, the formation of AgNPs is indicated by a color change to yellowish-brown [16]. The results of the synthesis show a color change, as shown in Figure 3.

Table 4. Phenolic content of TO-EE

Sample	Replication	Absorbance	Average absorbance	Initiating phenolic compound (mg/mL)	Total phenolics (mg GAE/g extract)
TO-EE	1	0.443	0.418	0.169	168.972
	2	0.417			
	3	0.395			

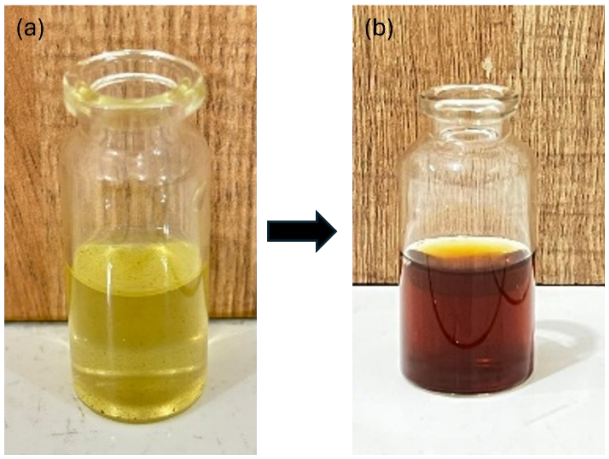

Figure 3. (a) $AgNO_3$ + TO-EE and (b) AgNPs-TO product

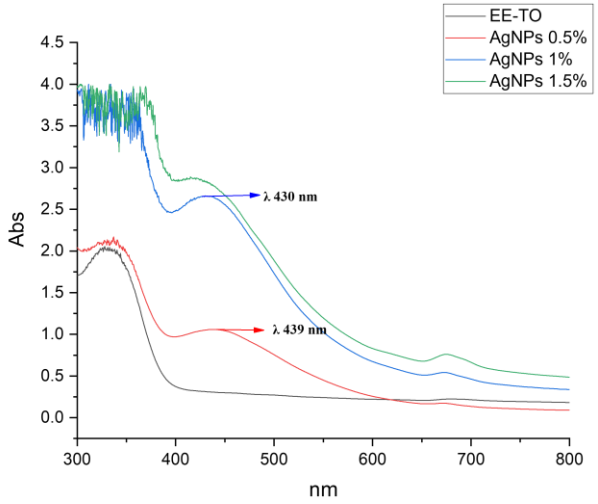

Figure 4. UV-Vis spectra of AgNPs-TO nanoparticles

3.4.2. Characterization of AgNPs Nanoparticles Using Fourier Transform Infrared Spectroscopy (FTIR)

The results of the FTIR characterization of the AgNPs-TO and TO-EE samples are shown in Figure 5. The FTIR spectrum shows that the 3570–3200 cm^{-1} wavelength range corresponds to the functional group of the hydroxyl group (-OH), which originates from phenolic and flavonoid compounds. The presence of the C-H functional group in TO-EE at 2926 cm^{-1} and in the wavelength range of 2935–2915 cm^{-1} indicates the presence of alkaloids and other compounds of secondary metabolites [29]. The presence of a band in the 1600–1700 cm^{-1} wavelength range is generally associated with carbonyl groups, especially when those groups are involved in hydrogen bonding or interacting with other molecules. According to Ningrum *et al.* [30], these groups indicate regions associated with C=O stretching vibrations in the amide structure.

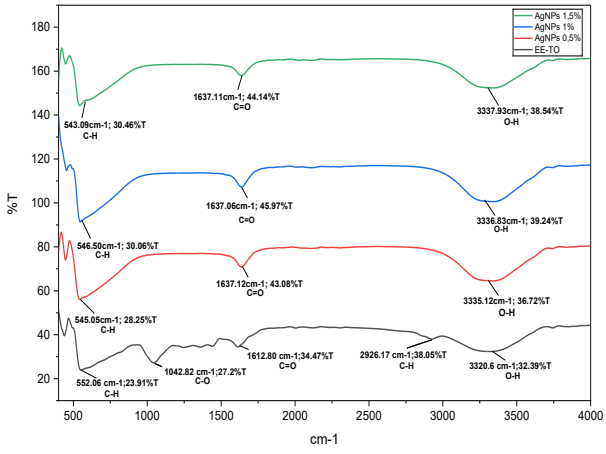

Figure 5. FTIR spectra of TO-EE and AgNPs-TO nanoparticles

In the synthesis of silver nanoparticles, these amide groups can interact or coordinate with metal ions, thereby playing a role in both the reduction process and the stabilization of the nanoparticles. Additionally, the functional groups on the resulting AgNPs show a shift in wavelength or even disappear compared to TO-EE. This is consistent with findings previously reported by Velgosova *et al.* [31]. This indicates that a bioreduction process is taking place and that secondary metabolites play a role in reducing Ag^+ to Ag^0.

3.4.3. Characterization Using a Particle Size Analyzer (PSA)

The AgNPs-TO nanoparticles were characterized using PSA to determine their particle size and polydispersity index (PDI) based on three replicate measurements, as shown in Figure 6. The results showed that AgNPs-TO had an average particle size (Z-average) of 56.46 ± 0.251 nm and a PDI of 0.594 ± 0.021, as can be seen in Table 5. The particle size of AgNPs-TO falls within the nanoparticle range of 1–100 nm [6]. Meanwhile, the relatively high PDI value indicates a broad particle-size distribution, suggesting that the particles are not highly uniform in size. Maulida *et al.* [32] reported that aggregation can occur during the synthesis of extract-mediated AgNPs, which is commonly observed in plant-mediated nanoparticle synthesis. This behavior may be associated with variations in the composition of bioactive compounds in the extract that act as reducing and stabilizing agents, as well as differences in nucleation and growth rates during nanoparticle formation. Furthermore, the particle size and stability of AgNPs can be influenced by biomolecules acting as capping agents and by synthesis parameters, including extract and $AgNO_3$ concentrations, temperature, and reaction time [33].

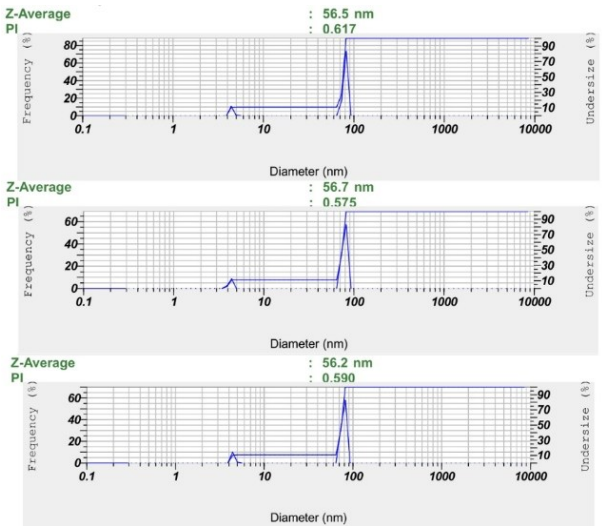

Figure 6. PSA results of AgNPs-TO

Table 5. Particle size and PDI of AgNPs-TO determined by PSA

Particle size	PDI
56.46 ± 0.251	0.594 ± 0.021

3.4.4. Transmission Electron Microscopy (TEM) Characterization

The results of the TEM analysis provide a visual representation of the AgNPs-TO product and are used to determine the size, shape, surface morphology, texture, and particle distribution. The AgNPs-TO product exhibits a spherical or round shape, as shown in Figure 7. The TEM characterization of AgNPs-TO showed an average particle size of 14.02 nm, indicating a broad distribution and suggesting polydispersity or non-uniform particle sizes. Based on findings from a study [34] that examined the differences between TEM and PSA/DLS, TEM measures the diameter of the metal core of nanoparticles, as this technique is sensitive to regions with high electron density. However, DLS measures the hydrodynamic diameter, which includes not only the metal core of the nanoparticles but also the capping agent layer and the solvent (hydration) layer adsorbed on the particle surface. This is also consistent with the observations reported by Khodeer *et al.* [35], whereby the AgNPs observed by TEM were smaller than those observed by PSA.

Variations in the size and shape of the nanoparticles may be caused by the presence of bioactive molecules from plant extracts that adsorb onto the particle surface, thereby playing a role in the formation and stabilization. A similar phenomenon was reported by Gaddam *et al.* [36] for AgNPs synthesized using *Drosera spatulata* Labill. var. *bakoensis* extract. This finding is further supported by the study conducted by Das *et al.* [10]. In the case of AgNPs synthesized using *T. orientalis* extract, the particle size ranged from 14.04 to 34.38 nm. As shown in Figure 7, the SAED pattern exhibits distinct concentric rings, indicating the crystalline nature of the AgNPs. The rings consist of numerous diffraction spots, suggesting that the nanoparticles are polycrystalline and contain multiple crystallites with different orientations.

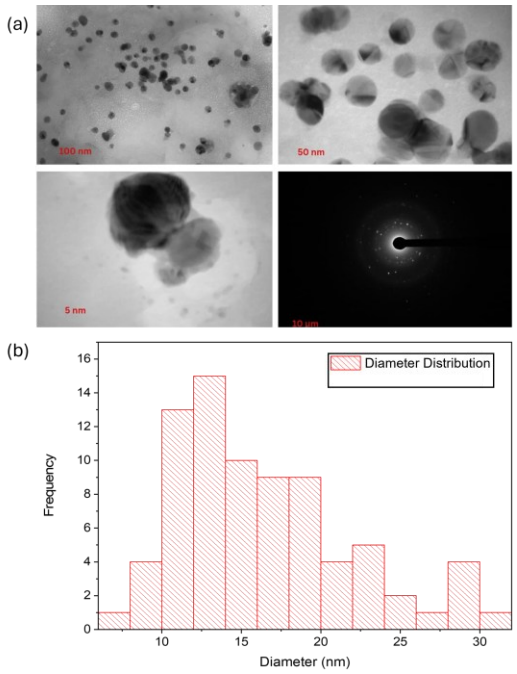

Figure 7. TEM characterization of AgNPs-TO: (a) TEM image and (b) particle size frequency distribution

3.4.5. Characterization Results from X-ray Diffraction (XRD)

Analysis of data from XRD of the AgNPs-TO product revealed 2θ peaks at 38.1°, 44.4°, and 64.5°, corresponding to (111), (200), and (220), indicating the presence of silver (Ag) in the AgNPs based on data from JCPDS no. 00-004-0783, and the diffraction peaks correspond to the crystal planes of the face-centered cubic (fcc) structure of metallic silver, indicating that the silver phase is the main component in the formation of silver nanoparticles through an environment-friendly synthesis [10], as shown in Figure 8.

AgCl peak appeared in the TO-EE-based AgNPs synthesis at diffraction peaks of 27.8°, 32.2°, 46.2°, 54.9°, 57.6°, and 67°. In accordance with the AgCl diffraction standard (ICCD card no. 31-1238), this indicates a cubic crystal structure [37]. According to a study by Dagher *et al.* [38], the presence of these AgCl crystals might be caused by impurities in the plant extract or by the use of a solvent that was not fully distilled, leading to the formation of AgCl as a result of a reaction between Ag^+ ions and Cl^- ions in small quantities during the biological synthesis of nanoparticles based on the plant extract, which was subsequently detected by XRD.

3.5. Antioxidant Test Using the DPPH Method

The antioxidant activity of TO-EE and AgNPs-TO was evaluated using the DPPH assay, and the corresponding IC_{50} values are presented in Table 6. AgNPs-TO exhibited an IC_{50} value of 128.404 µg/mL, which was higher than that of TO-EE (75.597 µg/mL), indicating lower DPPH radical-scavenging activity. However, the IC_{50} value of AgNPs-TO was lower than that of ascorbic acid. A similar finding was reported by Luhata *et al.* [39], who observed lower DPPH radical-scavenging activity for AgNPs synthesized using *O. strictum* extract and attributed this finding to the synthesis conditions.

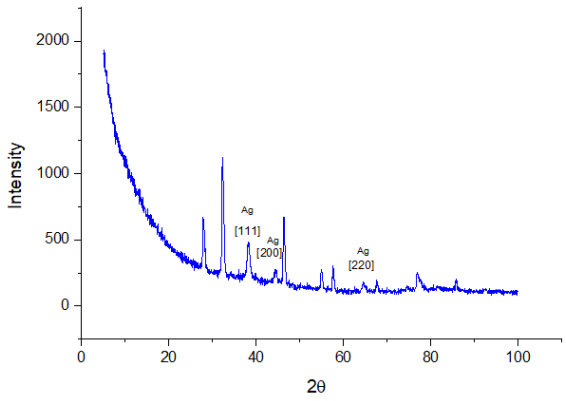

Figure 8. XRD pattern of AgNPs-TO

Table 6. Antioxidant activity of TO-EE and AgNPs-TO

Sample	IC_{50} (µg/mL)
TO-EE	75.598
AgNPs-TO	128.404
Ascorbic acid	12.087

During the green synthesis of AgNPs, phenolic and flavonoid compounds may contribute to the reduction of Ag^{+} to metallic Ag^{0} via their hydroxyl (–OH) groups and subsequently act as capping agents to stabilize the nanoparticles. Consequently, some of these bioactive compounds may be consumed during the reduction process or become associated with the nanoparticle surface, potentially reducing the availability of free functional groups involved in DPPH radical scavenging. This may contribute to the lower antioxidant activity observed for AgNPs-TO compared with TO-EE. In addition, changes or degradation of certain bioactive compounds during nanoparticle synthesis may further affect the antioxidant activity of the resulting AgNPs [40].

A similar finding was reported by Srećković *et al.* [41], who observed differences in the IC_{50} values between the extract and the corresponding AgNPs. According to Hanum *et al.* [42], antioxidant activity based on IC_{50} values can be classified as very strong (<50 mg/L), strong (50–100 mg/L), moderate (100–150 mg/L), weak (150– 200 mg/L), and very weak (>500 mg/L). Based on this classification, TO-EE, with an IC_{50} value of 75.597 µg/mL, is categorized as a strong antioxidant, whereas AgNPs-TO, with an IC_{50} value of 128.404 µg/mL, is categorized as a moderate antioxidant. These results indicate that both TO-EE and AgNPs-TO exhibit antioxidant activity, although TO-EE showed stronger DPPH radical-scavenging activity than AgNPs-TO.

3.6. Toxicity Test Results Using the BSLT Method

The toxicity test was conducted using the BSLT as an initial screening method to evaluate the toxicity of TO-EE and AgNPs-TO intended for use in active packaging. The LC_{50} values obtained were used to assess the toxicity levels of the tested materials. According to Pranata *et al.* [43], materials with an LC_{50} <30 µg/mL are classified as highly toxic; those with an LC_{50} <1000 µg/mL are classified as toxic; and those with an LC_{50} >1000 µg/mL are considered non-toxic. The LC_{50} results for TO-EE and AgNPs-TO are shown in Tables 7 and 8.

Table 7. BSLT results and LC_{50} value of TO-EE

Concentration (ppm)	Amount	Mortality (%)	LC_{50} (ppm)
0	0.00 ± 0.00	0.00	
100	0.33 ± 0.58	3.33	
250	1.00 ± 0.00	10.00	>1000
500	1.33 ± 0.58	13.33	
750	1.67 ± 0.58	16.67	
1000	2.33 ± 0.58	23.33	

Table 8. BSLT results for AgNPs-TO

Concentration (ppm)	Amount	Mortality (%)	LC_{50} AgNPs-TO
0	0.00 ± 0.00	0.00	
2.5	0.00 ± 0.00	0.00	
5	1.33 ± 0.58	13.33	35.64
10	2.33 ± 0.58	23.33	
25	3.33 ± 0.58	33.33	
50	6.00 ± 0.00	60	

The one-way ANOVA analysis results indicate that variations in extract concentration have a significant effect on *Artemia salina* mortality, as evidenced by an F- value of 10.00 and a p-value < 0.001. This indicates a significant difference among treatments, where an increase in extract concentration significantly affects larval mortality rates.

The AgNPs-TO results were similar to those of TO-EE, showing that variations in AgNPs concentration had a highly significant effect on the mortality of *Artemia salina larvae.* This was demonstrated by a calculated F-value of 94.20 with a p-value < 0.001, indicating a significant difference among the concentration treatments. Therefore, an increase in AgNPs concentration has a significantly different effect on larval mortality rates.

The BSLT results showed that AgNPs-TO had a lower LC_{50} than TO-EE, indicating greater toxicity toward Artemia salina larvae. Niranjan *et al.* [44] also reported similar findings, with in vivo toxicity tests in rats showing a relatively high tolerance to AgNPs at doses of up to >2000 mg/kg, although dose-dependent histopathological changes were observed in certain organs. In the context of the EFSA safe limit for AgNPs in food packaging, which is 10 mg/kg, a concentration of 5 µg/mL is still considered safe [45].

3.7. BP/AgNPs-TO Alginate-Based Biofilm

The visual examination of the biopolymer films containing AgNPs-TO at various concentrations generally showed a homogeneous appearance, ranging in color from transparent to slightly yellowish, and no significant cracks or macroscopic defects (Figure 9). This indicates that the addition of AgNPs-TO did not interfere with the overall formation of the biopolymer matrix.

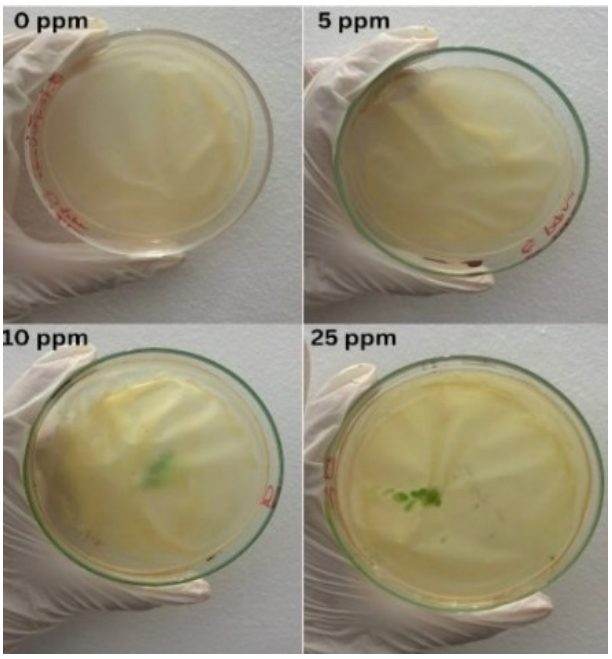

Figure 9. BP/AgNPs-TO biofilm product

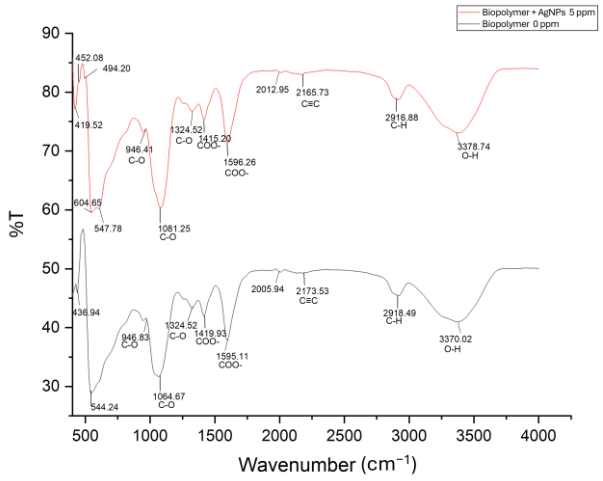

Figure 10. FTIR spectra of BP/AgNPs-TO

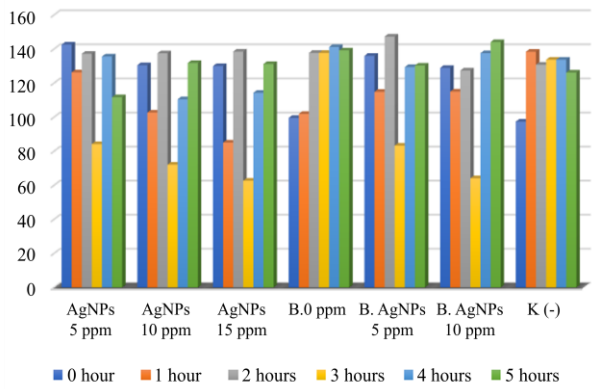

Figure 11. Antiphotooxidation results

According to the BSLT results, an AgNPs-TO concentration of 5 ppm was classified as safe and showed no significant toxic effects. Therefore, further FTIR analysis focused on biopolymer samples without AgNPs (0 ppm) and with AgNPs-TO at 5 ppm, representing the control and safe optimal conditions, respectively. The FTIR spectra showed the presence of –OH and COO^- groups, along with shifts in the bands toward lower wavenumbers. The absorption bands in the 400–1100 cm^{-1} range further confirmed the formation of AgNPs [46]. The FTIR spectra are presented in Figure 10.

3.8. Antiphotooxidation Test on Linoleic Acid

At the optimal wavelength of 232 nm, corresponding to conjugated diene formation [20], the results showed that the 15 ppm AgNPs-TO sample provided the most effective protection of the linoleic acid lipid system at the third hour, followed by the 10 ppm BP/AgNPs-TO sample. Compared with the negative control, the presence of bioactive compounds with antioxidant activity reduced the conjugated diene values [19].

All samples showed a downward trend at the third hour, indicating a temporary inhibition of hydroperoxide formation. After that time, the values increased again, indicating that the oxidation process continued over time. This may be due to the possibility that the bioactive capping agent compounds of AgNPs protecting the emulsion decreased over the course of the test, as shown in the diagram in Figure 11. Additionally, according to the literature [19], the higher values observed may be attributed to sample instability during testing or irregularities within the system.

3.9. Thickness, Water Absorption, and Tensile Strength of BP/AgNPs-TO

The physical characteristics of the BP/AgNPs-TO film, as determined by thickness measurements taken at three points, indicate that an increase in AgNPs concentration increases the biopolymer thickness to 133.3 mm (0.0133 cm). The thickness of the biopolymer is influenced by its solid content. The results meet the Japanese Industrial Standard (<0.025 cm) [22], as shown in Figure 12.

The water absorption of the biopolymer films increased with increasing AgNPs-TO concentration, with the highest value observed at 25 ppm. The relatively high water absorption of the films can be attributed to the inherently hydrophilic nature of the alginate/PEG matrix. Alginate contains abundant hydroxyl and carboxyl groups [47], while PEG is also hydrophilic and may further enhance water absorption. Similar observations were reported for silver–alginate nanocomposite films, where the addition of AgNPs resulted in a rough and porous film morphology [48]. The relatively low concentration of $CaCl_2$ used for the cross-linking process may also contribute to the high water absorption rate.

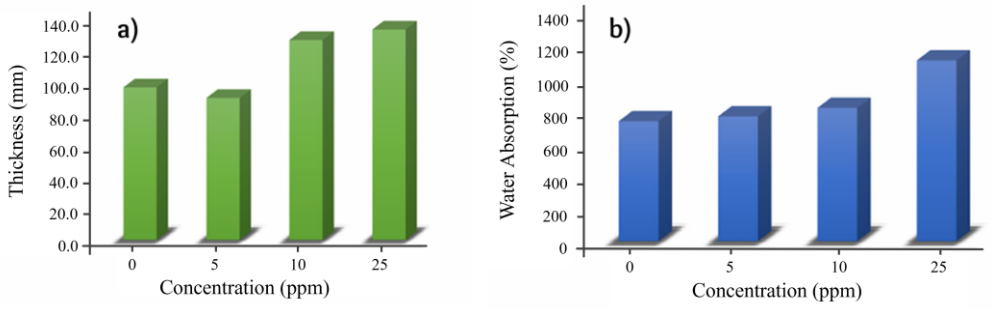

Figure 12. (a) Water absorption and (b) BP/AgNPs-TO thickness diagrams

Table 9. Tensile strength of BP/AgNPs-TO

Sample (ppm)	Tensile strength (MPa)
0	20.14
5	5.15

The tensile testing results of the BP/AgNPs-TO biofilm showed that the tensile strength decreased from 20.1 MPa without AgNPs (0 ppm) to 5.15 MPa with the addition of 5 ppm AgNPs-TO, as shown in Table 9. This decrease indicates that the presence of silver nanoparticles affected the mechanical properties of the biopolymer film. The reduced tensile strength may be attributed to disrupted interactions between polymer chains due to the presence of AgNPs in the film matrix. This finding is consistent with previous research [48], which reported that the incorporation of AgNPs can reduce intermolecular interactions between alginate chains. The film without AgNPs exhibited the highest tensile strength, indicating that the presence of AgNPs may weaken the interactions between alginate biopolymer chains.

The low tensile strength of the BP/AgNPs-TO film with 5 ppm AgNPs is likely due to the uneven distribution of nanoparticles resulting from agglomeration within the alginate matrix. This is supported by the PSA results, which showed a PDI greater than 0.5, indicating a broad particle size distribution and a tendency toward nanoparticle agglomeration, which may lead to the heterogeneous dispersion of AgNPs within the biopolymer matrix. This condition causes the mechanical properties of the film to be inconsistent across different sections [48].

4. Conclusion

Based on the results of this study, the AgNPs-TO nanoparticle product was successfully synthesized using an environmentally friendly method. The success of the synthesis was confirmed by characterization, namely through the appearance of a UV-Vis absorption peak at 430 nm, changes in functional groups in the FT-IR spectrum, an average particle size of 56.46 nm with a PDI of 0.594, and spherical particle morphology with a heterogeneous distribution. Analysis of XRD revealed characteristic peaks of metallic silver with a face-centered cubic (fcc) crystal structure. The resulting AgNPs-TO exhibited good antioxidant activity and anti-photooxidation capabilities when applied to active biopolymer films, with optimal results at a concentration of 15 ppm and a BP/AgNPs-TO ratio of 10 ppm. Based on the preliminary results of the BSLT test, the 5 ppm AgNPs formulation was selected as the optimal formulation due to its relatively low acute toxicity, satisfactory mechanical properties, and its effective ability to inhibit lipid photooxidation. Additionally, the addition of AgNPs also affects the physical characteristics of the film, particularly by increasing film thickness and water absorption, while decreasing tensile strength. Future studies should optimize the AgNPs concentration and film formulation to improve mechanical properties and nanoparticle dispersion, while migration and cytotoxicity studies are needed to ensure the safety of AgNP-based biopolymer films for food packaging applications. Thus, *T. orientalis* leaves have the potential to be utilized as a natural bioreductant and can be applied for the development of environmentally friendly food packaging.

Acknowledgment

The author would like to thank the Ministry of Higher Education, Science, and Technology of the Republic of Indonesia (Kemendiktisaintek) for the funding support provided under the 2025 Student Creativity Program (PKM-RE), which enabled this research to be successfully carried out. Gratitude is also extended to the Chemistry Laboratory of the University of Muhammadiyah Riau (UMRI) for the facilities and technical support provided during the research. Furthermore, the author is grateful for the contributions from the Electron Microscopy Laboratory at the Bandung Institute of Technology (ITB) and the Chemistry Laboratory at Padang State University (UNP) for their assistance in the sample characterization process, which significantly supported the completeness of the data in this study.

References

[1] Milie Diarty, Arie Wahyu Wijayanto, Analisis Aspek Ketahanan Pangan Indonesia dengan *Hard* dan *Soft Clustering*, *Rekayasa*, 17, 1, (2024), 108-123 https://doi.org/10.21107/rekayasa.v17i1.21774

[2] Lalu Moh. Arsal Fadila, Nadia Arsyta Putri, Analisis Perkembangan Ketahanan Pangan di Indonesia: Pendekatan Menggunakan Big Data dan Data Mining, *Seminar Nasional Official Statistics*, 2023 https://doi.org/10.34123/semnasoffstat.v2023i1.1890

[3] Octavia Trisna Mahardani, Leny Yuanita, Efek Metode Pengolahan dan Penyimpanan terhadap Kadar Senyawa Fenolik dan Aktivitas Antioksidan,

UNESA Journal of Chemistry, 10, 1, (2021), 64-78 https://doi.org/10.26740/ujc.v10n1.p64-78

[4] Susana Guzman-Puyol, Jesús Hierrezuelo, José J. Benítez, Giacomo Tedeschi, José M. Porras-Vázquez, Antonio Heredia, Athanassia Athanassiou, Diego Romero, José A. Heredia-Guerrero, Transparent, UV-blocking, and high barrier cellulose-based bioplastics with naringin as active food packaging materials, *International Journal of Biological Macromolecules*, 209, (2022), 1985-1994 https://doi.org/10.1016/j.ijbiomac.2022.04.177

[5] Bangaru Babu Alampally, Y. Subba Rao, Sravanthi Pidamarthi, Sankara Rao Miditana, Pulsingh Dhanavath, Durga Bhavani A.K., Green synthesis of silver nanoparticles using *Azadirachta indica* (Neem) fruit pulp extract and their antioxidant, antibacterial, and anticancer activity, *Sustainable Chemistry for the Environment*, 11, (2025), 100282 https://doi.org/10.1016/j.scenv.2025.100282

[6] Qudsia Sarwer, Muhammad Shoaib Amjad, Ansar Mehmood, Zakia Binish, Ghazala Mustafa, Atikah Farooq, Mirza Faisal Qaseem, Fozia Abasi, José Manuel Pérez de la Lastra, Green Synthesis and Characterization of Silver Nanoparticles Using *Myrsine africana* Leaf Extract for Their Antibacterial, Antioxidant and Phytotoxic Activities, *Molecules*, 27, 21, (2022), 7612 https://doi.org/10.3390/molecules27217612

[7] Danaja Štular, Elisa Savio, Barbara Simončič, Matic Šobak, Ivan Jerman, Ida Poljanšek, Ada Ferri, Brigita Tomšič, Multifunctional antibacterial and ultraviolet protective cotton cellulose developed by *in situ* biosynthesis of silver nanoparticles into a polysiloxane matrix mediated by sumac leaf extract, *Applied Surface Science*, 563, (2021), 150361 https://doi.org/10.1016/j.apsusc.2021.150361

[8] Sefelin Sefelin, Sri Royani, Dian Islamiyati, Green Synthesis Nanopartikel Perak Menggunakan Ekstrak Daun Pepaya (*Carica papaya* L.), *Insologi: Jurnal Sains dan Teknologi*, 4, 6, (2025), 1627-1635 https://doi.org/10.55123/insologi.v4i6.6859

[9] D. Niranjan, N. Shridhar, M. Vinuta, S. Manjunatha, U. Sunilchandra, B. Pradeep, G. Manju, P. S. Revanna, Botanical, pharmacological and toxicological properties of *Trema orientalis*: A Review, *Journal of Phytopharmacology*, 12, 6, (2023), 392-398 https://doi.org/10.31254/phyto.2023.12605

[10] Richa Das, Pradeep Kumar, Amit Kumar Singh, Shreni Agrawal, Salim Albukhaty, Indrani Bhattacharya, Kavindra Nath Tiwari, Sunil Kumar Mishra, Amit Kumar Tripathi, Faizah A. AlMalki, Azalldeen Kazal Alzubaidi, Wasan J. Al-Kaabi, Vishnu D. Rajput, Zaidon T. Al-aqbi, Green synthesis of silver nanoparticles using *Trema orientalis* (L.) extract and evaluation of their antibacterial activity, *Green Chemistry Letters and Reviews*, 18, 1, (2025), 2444679 https://doi.org/10.1080/17518253.2024.2444679

[11] Apparao Gudimalla, Jiya Jose, Rajendran Jose Varghese, Sabu Thomas, Green Synthesis of Silver Nanoparticles Using *Nymphae odorata* Extract Incorporated Films and Antimicrobial Activity, *Journal of Polymers and the Environment*, 29, (2021), 1412-1423 https://doi.org/10.1007/s10924-020-01959-6

[12] Aiste Balciunaitiene, Viktorija Januskevice, Sandra Saunoriute, Urte Raubyte, Jonas Viskelis, Patrick B. Memvanga, Pranas Viskelis, Antimicrobial Antioxidant Polymer Films with Green Silver Nanoparticles from *Symphyti radix*, *Polymers*, 16, 3, (2024), 317 https://doi.org/10.3390/polym16030317

[13] Noverda Ayuchecaria, Efriyana Oksal, Natalia Sri Martani, Nisa Kartika Komara, Chuchita, Zimon Pereiz, Skrining Fitokimia dan Uji Antibakteri Ekstrak Etanol Daun Hanjuang Merah (*Cordyline fruticose*) Terhadap Bakteri *Staphylococcus epidermidis*, *Jurnal Insan Farmasi Indonesia*, 7, 1, (2024), 86-94 https://doi.org/10.36387/jifi.v7i1.1683

[14] Jerome Eberhardt, Diogo Santos-Martins, Andreas F. Tillack, Stefano Forli, AutoDock Vina 1.2.0: New Docking Methods, Expanded Force Field, and Python Bindings, *Journal of Chemical Information and Modeling*, 61, 8, (2021), 3891-3898 https://doi.org/10.1021/acs.jcim.1c00203

[15] Abhishek Tripathi, Kapali Suri, Sriram K., N. Arul Murugan, Assessing the accuracy of binding pose prediction for kinase proteins and 7-azaindole inhibitors: a study with AutoDock4, Vina, DOCK 6, and GNINA 1.0, *RSC Advances*, 15, 55, (2025), 47051-47065 https://doi.org/10.1039/d5ra05526a

[16] Dias Wahyu Arvian, Ismi Rahmawati, Endang Diyah Ikasari, Green Synthesis of Silver Nanoparticles of Leaf Extract of Senduduk Bulu (*Clidemia hirta* (L.) D. Don) and Exploration of the Antibacterial Activity, *MEDFARM: Jurnal Farmasi dan Kesehatan*, 14, 1, (2025), 79-95 https://doi.org/10.48191/medfarm.v14i1.574

[17] Haiyul Fadhli, Hefriza Putri, Aktivitas Antioksidan dan Profil Fitokimia Ekstrak Metanol Daun *Bauhinia purpurea* L. dari Pekanbaru, *Jurnal Farmasi Indonesia*, 18, 1, (2026), 10-18

[18] Gabriella Cantika Vidi, Putri Vidiasari Darsono, Rahmadani Rahmadani, Toksisitas Ekstrak Daun Sungkai (*Peronema canescens* Jack) Terhadap Larva *Artemia salina Leach* dengan Metode *Brine Shrimp Lethality Test* (BSLT), *Jurnal Surya Medika*, 10, 2, (2024), 129-136 https://doi.org/10.33084/jsm.v10i2.7734

[19] Tegar Pelealu, Edi Suryanto, Meiske Sientje Sangi, Aktivitas Antifotooksidasi dan Tabir Surya Ekstrak dan Fraksi Pelarut dari Daun Gamal (*Gliricidia sepium*), *Chemical Progress*, 16, 1, (2023), 71-78 https://doi.org/10.35799/cp.16.1.2023.47202

[20] Jamila Gagour, Otmane Hallouch, Abderrahim Asbbane, Abdellatif Laknifli, El Hassan Sakar, Khalid Majourhat, Said Gharby, Physicochemical Characterization of 'Moroccan Picholine' Olive (*Olea europaea* L.) Oil Produced in Southern Morocco Using Multivariate Statistical Analysis, *Analytica*, 5, 1, (2024), 119-138 https://doi.org/10.3390/analytica5010008

[21] Ludmila Motelica, Denisa Ficai, Ovidiu-Cristian Oprea, Anton Ficai, Vladimir-Lucian Ene, Bogdan-Stefan Vasile, Ecaterina Andronescu, Alina-Maria Holban, Antibacterial Biodegradable Films Based on Alginate with Silver Nanoparticles and Lemongrass Essential Oil–Innovative Packaging for Cheese, *Nanomaterials*, 11, 9, (2021), 2377 https://doi.org/10.3390/nano11092377

[22] Khusnul Khotimah, Ali Ridlo, Chrisna Adhi Suryono, Sifat Fisik dan Mekanik Bioplastik Komposit dari Alginat dan Karagenan, *Journal of Marine Research*, 11, 3, (2022), 409-419 https://doi.org/10.14710/jmr.v11i3.33865

[23] Sri Hilma Siregar, P. Prasetya, Aulia Rizki Ramadhanti, Rian Putra, Siti Zahidah, Eco-friendly Edible Film from Chicken Bone Waste and Tapioca Starch, *Jurnal Kimia Sains dan Aplikasi*, 25, 2, (2022), 79-86 https://doi.org/10.14710/jksa.25.2.79-86

[24] Jerzy Bochnia, Malgorzata Blasiak, Tomasz Kozior, Tensile Strength Analysis of Thin-Walled Polymer Glass Fiber Reinforced Samples Manufactured by 3D Printing Technology, *Polymers*, 12, 12, (2020), 2783 https://doi.org/10.3390/polym12122783

[25] Omokehinde F. Taiwo, Abiodun H. Adebayo, Joseph A. O. Olugbuyiro, Phytochemical and Antioxidant Studies of *Albizia zygia* (DC.) J.F. Macbride and *Trema orientalis* (Linn.) Blume, *African Journal of Biomedical Research*, 27, 3, (2024), 206-216

[26] Nasrin Jubayda, Md. Tanveer Ahsan, Md. Kaisar Alam, T. S. Farah Mousumi, Tanbirul Azim Maharaj, Mohammad Arman, Integrated Phytochemical, Pharmacological, and In Silico Evaluation of the Methanolic Extract of *Cayratia trifolia* Leaves: Antioxidant, Anti-Inflammatory, and Analgesic Activities, *The Scientific World Journal*, 2026, 1, (2026), 8390762 https://doi.org/10.1155/tswj/8390762

[27] Juliana Sihombing, Muhammad Yunus, Finna Piska, Uji Aktivitas Antioksidan dan Profil Kandungan Fenol serta Flavonoid pada Ekstrak Daun Sirsak (*Annona muricata* L.), *Jurnal Ilmiah Penelitian Mahasiswa*, 4, 1, (2026), 1265-1272

[28] Rachmin Munadi, Endah Dwijayanti, Nolfi Febrianto, Biosintesis Nanopartikel Perak dari *Hylocereus polyrhizus* dan Uji Sensitifitas serta Selektifitasnya Terhadap Logam Berat, *Cokroaminoto Journal of Chemical Science*, 7, 1, (2025), 1-6

[29] Satria Putra Jaya Negara, Hasri, Andi Eka Kartika, Green Synthesis Nanopartikel Perak Menggunakan Ekstrak Bunga Telang (*Clitoria ternatea*) dan Karakterisasinya, *Journal of Sustainable Innovation on Education, Mathematics and Natural Sciences*, 5, 2, (2026), 332-340 https://doi.org/10.53696/venn.v5i2.436

[30] Dinda Alithia Ningrum, Khairiza Lubis, Dinda Syahfitri, Dhifa Umairoh Putri, Cyndi Clodia, Hanifah Dzaky Fadillah, Gita Hartati, Sintesis dan Karakterisasi Nanopartikel Perak Ekstrak Daun Melinjo (*Gnetum gnemon* L.) serta Potensinya sebagai Antibakteri, *Journal of Biological Sciences*, 13, 1, (2026), 39-54 https://doi.org/10.24843/metamorfosa.2026.v13.i01.p4

[31] Oksana Velgosova, Silvia Dolinská, Helena Podolská, Lívia Mačák, Elena Čižmárová, Impact of Plant Extract Phytochemicals on the Synthesis of Silver Nanoparticles, *Materials*, 17, 10, (2024), 2252 https://doi.org/10.3390/ma17102252

[32] Alifiani Maulida, Gusrizal Gusrizal, Anis Shofiyani, Kitolod (*Isotoma longiflora* Presl) Leaf Extract as a Bioreductor in Silver Nanoparticle, *ALCHEMY Jurnal Penelitian Kimia*, 22, 1, (2026), 127-137 https://doi.org/10.20961/alchemy.22.1.109231.127-137

[33] Chhangte Vanlalveni, Samuel Lallianrawna, Ayushi Biswas, Manickam Selvaraj, Bishwajit Changmai, Samuel Lalthazuala Rokhum, Green synthesis of silver nanoparticles using plant extracts and their antimicrobial activities: a review of recent literature, *RSC Advances*, 11, 5, (2021), 2804-2837 https://doi.org/10.1039/d0ra09941d

[34] Ana M. Ferreira, Anna Vikulina, Michael Loughlin, Dmitry Volodkin, How similar is the antibacterial activity of silver nanoparticles coated with different capping agents?, *RSC Advances*, 13, 16, (2023), 10542-10555 https://doi.org/10.1039/d3ra00917c

[35] Dina M. Khodeer, Ali M. Nasr, Shady A. Swidan, Sarah Shabayek, Roaa M. Khinkar, Mohammed M. Aldurdunji, Maryam A. Ramadan, Jihan M. Badr, Characterization, antibacterial, antioxidant, antidiabetic, and anti-inflammatory activities of green synthesized silver nanoparticles using *Phragmanthera austroarabica* A. G. Mill and J. A. Nyberg extract, *Frontiers in Microbiology*, 13, (2023), 1078061 https://doi.org/10.3389/fmicb.2022.1078061

[36] Susmila Aparna Gaddam, Venkata Subbaiah Kotakadi, Gunasekhar Kalavakunta Subramanyam, Josthna Penchalaneni, Varadarajulu Naidu Challagundla, Sai Gopal D. V. R., Visweswara Rao Pasupuleti, Multifaceted phytogenic silver nanoparticles by an insectivorous plant *Drosera spatulata* Labill var. bakoensis and its potential therapeutic applications, *Scientific Reports*, 11, (2021), 21969 https://doi.org/10.1038/s41598-021-01281-8

[37] A. M. Abdel-Hafeez, Mahmoud Abdel-Halim Abdel-Goad, Green synthesis of Ag/AgCl nanoparticles using Jatropha seed extract for photocatalytic degradation and antibacterial treatment of petroleum industry wastewater, *Discover Sustainability*, 6, (2025), 906 https://doi.org/10.1007/s43621-025-01139-3

[38] Wael Dagher, Abeer Alassod, Mhd Firas Al Hinnawi, Ibrahim Alghoraibi, Amal Taher, Manal Alnhlaoui, Characterization and antibacterial effect of green-synthesised silver nanoparticles using different extraction methods from *Ziziphus spina-christi* (Sidr) leaf extract collected from Syria, *RSC Advances*, 15, 42, (2025), 35642-35659 https://doi.org/10.1039/d5ra05214a

[39] Lokadi Pierre Luhata, Christian Nanga Chick, Natsuki Mori, Kunihito Tanaka, Hiroshi Uchida, Takashi Hayashita, Toyonobu Usuki, Synthesis and Antioxidant Activity of Silver Nanoparticles Using the *Odontonema strictum* Leaf Extract, *Molecules*, 27, 10, (2022), 3210 https://doi.org/10.3390/molecules27103210

[40] Abdur Rahman, Zulqarnain Zulqarnain, Khizar Hayat, Nasir Assad, Muhammad Nauman Khan, Misbah Zia, Nirvana Iqbal, Alevcan Kaplan, Shabab Hussain, Dalya Marwan Attallah, Jawahir A. Mokhtar, Maged Mostafa Mahmoud, Phytomediated synthesis of silver nanoparticles using *Fumaria indica* extract with antibacterial, antifungal and antioxidant properties, *Discover Sustainability*, 7, (2026), 399 https://doi.org/10.1007/s43621-026-02837-2

[41] Nikola Z. Srećković, Zoran P. Nedić, Davide Liberti, Daria Maria Monti, Nevena R. Mihailović, Jelena S. Katanić Stanković, Silvana Dimitrijević, Vladimir B. Mihailović, Application potential of biogenically synthesized silver nanoparticles using *Lythrum salicaria* L. extracts as pharmaceuticals and catalysts for organic pollutant degradation, *RSC Advances*, 11, 56, (2021), 35585-35599 https://doi.org/10.1039/d1ra05570d

[42] Rahma Farida Hanum, Enny Fachriyah, Ismiyarto Ismiyarto, Purbowatiningrum Ria Sarjono, Total Phenolic Content Analysis, Antioxidant Activity, and Isolation of Phenolic Acid Compounds from Methanol Extract of Celery (*Apium graveolens* L.), *Jurnal Kimia Sains dan Aplikasi*, 28, 7, (2025), 345-354 https://doi.org/10.14710/jksa.28.7.345-354

[43] Guswarni Pranata, Indriaty Indriaty, Ekariana S. Pandia, Uji Kadar Total Tanin dari Ekstrak Daun Sembung (*Blumea balsamifera*) serta Toksisitasnya Dengan Metode BSLT, *Jurnal Sosial dan Sains*, 5, 6, (2025), 1703-1712 https://doi.org/10.59188/jurnalsosains.v5i6.32260

[44] D. Niranjan, N. B. Shridhar, M. H. Vinuta, S. S. Manjunatha, U. Sunilchandra, B. S. Pradeep, G. U. Manju, Patel Suresh Revanna, Toxicological Evaluation of *Trema orientalis* in Rats with Reference to Histopathology of Certain Tissues, *Biological Forum*, 15, 8a, (2023), 317-325

[45] Wenxi Yu, Qin Lei, Jingxian Jiang, Jianwei Yan, Xijian Yi, Juan Cheng, Siyu Ou, Wenjia Yin, Ziyan Li, Yuru Liao, Green-Synthesized Silver Nanoparticle-Loaded Antimicrobial Films: Preparation, Characterization, and Food Preservation, *Foods*, 14, 14, (2025), 2509 https://doi.org/10.3390/foods14142509

[46] Kamal Kayed, Mayada Issa, Hammoud Al-Ourabi, The FTIR spectra of Ag/Ag_2O composites doped with silver nanoparticles, *Journal of Experimental Nanoscience*, 19, 1, (2024), 2336227 https://doi.org/10.1080/17458080.2024.2336227

[47] Shenbagaraman Akshaya, Arputharaj Joseph Nathanael, A Review on Hydrophobically Associated Alginates: Approaches and Applications, *ACS Omega*, 9, 4, (2024), 4246-4262 https://doi.org/10.1021/acsomega.3c08619

[48] Endang Susilowati, Lina Mahardiani, Retno Duwi Hardini, The effect of silver nanoparticles toward properties and antibacterial activity of silver-alginate nanocomposite films, *Frontiers in Sustainable Food Systems*, 6, (2022), 913750 https://doi.org/10.3389/fsufs.2022.913750